Secondary ice production: current state of the science and recommendations for the future

Chapter 7

Secondary Ice Production: Current State of the Science and Recommendations for the Future

P. R. FIELD,[a,b] R. P. LAWSON,[c] P. R. A. BROWN,[a] G. LLOYD,[d] C. WESTBROOK,[e] D. MOISSEEV,[f] A. MILTENBERGER,[b] A. NENES,[g] A. BLYTH,[b] T. CHOULARTON,[d] P. CONNOLLY,[d] J. BUEHL,[h] J. CROSIER,[d] Z. CUI,[b] C. DEARDEN,[d] P. DEMOTT,[i] A. FLOSSMANN,[j] A. HEYMSFIELD,[k] Y. HUANG,[b] H. KALESSE,[h] Z. A. KANJI,[l] A. KOROLEV,[m] A. KIRCHGAESSNER,[n] S. LASHER-TRAPP,[o] T. LEISNER, G. MCFARQUHAR,[o] V. PHILLIPS,[p] J. STITH,[q] AND S. SULLIVAN[r]

[a] *Met Office, Exeter, United Kingdom*
[b] *Institute for Climate and Atmospheric Science, School of Earth and Environment, University of Leeds, Leeds, United Kingdom*
[c] *SPEC Inc., Boulder, Colorado*
[d] *School of Earth and Environmental Sciences, University of Manchester, Manchester, United Kingdom*
[e] *Department of Meteorology, University of Reading, Reading, United Kingdom*
[f] *Department of Physics, University of Helsinki, Helsinki, Finland*
[g] *School of Earth and Atmospheric Sciences, Georgia Institute of Technology, Atlanta, Georgia*
[h] *Leibniz Institute for Tropospheric Research, Leipzig, Germany*
[i] *Department of Atmospheric Science, Colorado State University, Fort Collins, Colorado*
[j] *Blaise Pascal University, Clermont-Ferrand, France*
[k] *NCAR, Boulder, Colorado*
[l] *Institute for Atmospheric and Climate Science, ETH Zurich, Zurich, Switzerland*
[m] *Environment and Climate Change Canada, Toronto, Canada*
[n] *British Antarctic Survey, Cambridge, United Kingdom*
[o] *Department of Atmospheric Sciences at the University of Illinois at Urbana–Champaign, Urbana, Illinois*
[p] *Department of Physical Geography and Ecosystem Science, Lund University, Lund, Sweden*
[q] *Earth Observing Laboratory, NCAR, Boulder, Colorado*
[r] *School of Chemical and Biomolecular Engineering, Georgia Institute of Technology, Atlanta, Georgia*

ABSTRACT

Measured ice crystal concentrations in natural clouds at modest supercooling (temperature $\sim > -10°C$) are often orders of magnitude greater than the number concentration of primary ice nucleating particles. Therefore, it has long been proposed that a secondary ice production process must exist that is able to rapidly enhance the number concentration of the ice population following initial primary ice nucleation events. Secondary ice production is important for the prediction of ice crystal concentration and the subsequent evolution of some types of clouds, but the physical basis of the process is not understood and the production rates are not well constrained. In November 2015 an international workshop was held to discuss the current state of the science and future work to constrain and improve our understanding of secondary ice production processes. Examples and recommendations for in situ observations, remote sensing, laboratory investigations, and modeling approaches are presented.

1. Introduction

Airborne observations of ice crystal concentrations are often found to exceed the concentration of ice nucleating particles (INPs) by many orders of magnitude (see, e.g., Mossop 1985; Hobbs and Rangno 1985; Beard 1992; Pruppacher and Klett 1997; Hobbs and Rangno 1998; Cantrell and Heymsfield 2005; DeMott et al. 2016). In the 1970s (Mossop et al. 1970; Hallett and Mossop 1974) the discrepancy between expected ice particle concentrations formed through primary ice nucleation and observed ice particle

Corresponding author e-mail: Paul Field, paul.field@metoffice.gov.uk

DOI: 10.1175/AMSMONOGRAPHS-D-16-0014.1

concentration motivated the search for mechanisms that could amplify primary nucleation pathways. These include thermophoretically enhanced contact freezing (Beard 1992; Young 1974; Hobbs and Rangno 1985), pre-activated INPs (Beard 1992; Fridlind et al. 2007), or a new, poorly understood, physical process capable of creating new ice crystals. The latter became known as secondary ice production (SIP). SIP is a mechanism or process that produces new ice crystals in the presence of preexisting ice without requiring the action of an ice nucleating particle (or homogeneous freezing).

Increasingly sophisticated cloud microphysical representations (e.g., Morrison et al. 2005; Seifert and Beheng 2006; Saleeby and van den Heever 2013; Thompson and Eidhammer 2014) are being used in numerical weather prediction (NWP) and global climate models (GCMs) to provide more realistic simulations of clouds. This drive toward greater complexity is motivated by the recognition of the importance of microphysical processes for the evolution of clouds, precipitation and the atmospheric environment. Some bulk microphysical representations used in models are now capable of predicting two moments of size distributions, namely the total number concentration as well as mass mixing ratio. Thus, one important challenge for the successful implementation of cloud microphysics is the accurate prediction of ice crystal concentrations. While the understanding and quantification of primary ice nucleation has experienced a renaissance in recent years (e.g., DeMott et al. 2011), SIP is a process that has received less attention but is potentially important for controlling the ice crystal concentrations found in some types of clouds. Consequently, the results from the initial ground breaking work done in the 1970s on SIP are still found in present-day cloud models.

There are a number of SIP mechanisms that have been described in the literature. Table 7-1 and Fig. 7-1 introduce the different types that will be referred to throughout the rest of the article.

The aims of this article are 1) to summarize the laboratory investigations and field observations (in situ and remote sensing) of SIP along with a review of modeling studies, and 2) to provide recommendations for future research aimed at understanding and constraining the SIP.

2. Laboratory evidence for SIP

a. Rime splintering and the Hallett–Mossop process

Initial investigations into SIP in the laboratory revolved around speculation dating back to the 1940s that ice splintering associated with the riming process was an important phenomenon (Hallett and Mossop 1974; Brewer and Palmer 1949; Findeisen and Findeisen 1943). To simulate rime splintering, an ice-coated cylinder, used to represent a large riming ice particle, was rapidly rotated within a cold box populated with supercooled liquid droplets (Hallett and Mossop 1974). It was found that for a certain range of temperature, droplet impact velocity, and size characteristics, numerous splinters of ice were generated. This has since been known as the Hallett–Mossop process (H-M). This process has received the most attention and evaluation over the past 40 years. All of the laboratory experiments documented in the literature that have employed this experimental setup have been successful in producing secondary ice (Hallett and Mossop 1974; Choularton et al. 1980; Heymsfield and Mossop 1984; Saunders and Hosseini 2001). However, attempts to explain or at least describe the physics underlying the mechanism itself have led to conflicting results.

The consensus is that H-M occurs within a temperature range of approximately $-3°$ to $-8°$C, in the presence of liquid cloud droplets smaller than $\sim 13\,\mu$m and liquid drops larger than $\sim 25\,\mu$m in diameter that can freeze when they are collected by large ice particles (rimed aggregates, graupel, or large frozen drops). An example of the determination of the temperature dependence of the process is shown in Fig. 7-2 (from Heymsfield and Mossop 1984). Originally it was speculated that symmetric freezing of supercooled droplets accreting on large ice particles results in a buildup of internal pressure in the freezing droplet, which is relieved by a crack in the frozen shell through which the unfrozen liquid escapes, producing a protuberance that can break up into splinters (Visagie 1969; Mossop et al. 1974). Griggs and Choularton (1983) suggested that an ice shell is too strong to break at temperatures $<-8°$C due to rapid growth. Mason (1996) supported this with theoretical calculations. Dong and Hallett (1989) found for temperatures $> -8°$C that droplets spread over the surface and did not form individual spherical ice. They suggested that thermal shock caused splintering due to the temperature gradient between substrate and drop. Based on laboratory results, Choularton et al. (1980) suggest that a large drop ($>\sim 25\,\mu$m) is more likely to freeze symmetrically and produce splinters when it falls on a small ($<\sim 13\,\mu$m) droplet that provides a narrow neck at the attachment point, limiting thermal contact. Various researchers have investigated the effects of relative velocity between the large ice and the accreted drops. For example, Mossop (1985) extended the low-velocity limit down to $0.2\,\mathrm{m\,s^{-1}}$ with a peak splinter production rate when the relative velocity is in the range of 2 to $4\,\mathrm{m\,s^{-1}}$. Later, Saunders and Hosseini (2001) found that the maximum splinter production peaks at a rimer collision velocity of $6\,\mathrm{m\,s^{-1}}$. Heymsfield and Mossop (1984) suggested that the peak splinter production depends on the surface temperature of the large ice particle rather than on cloud temperature.

TABLE 7-1. Secondary ice production mechanisms.

SIP	Description	Example references	Modeling implementation	Example model references
Rime splintering	Splinter production associated with riming process. Rimer could be graupel, large frozen drop, or snowflake.	Findeisen and Findeisen 1943	Splinter production rate dependent upon mass of supercooled liquid accreted.	Scott and Hobbs 1977; Beheng 1987; Aleksić 1989; Mason 1996; Blyth and Latham 1997; Ovtchinnikov and Kogan 2000; Phillips et al. 2001; Clark et al. 2005; Connolly et al. 2006b; Fridlind et al. 2007; Phillips et al. 2007; Huang et al. 2008; Crawford et al. 2012; Dearden et al. 2016
	Hallett–Mossop process: Special case of rime splintering. Splinter production demonstrated in the laboratory analog (ice covered rod) of graupel riming. Active in −3 to −8°C temperature range, requires a 0.2–5 m s^{-1} impaction speed and the presence of droplets exceeding 23 μm in diameter. The terms "rime splintering" and "Hallett–Mossop" are often used interchangeably in the literature.	Hallett and Mossop 1974	Splinter production rate dependent upon number of droplets collected. A variety of size thresholds are used including larger than 25 microns and smaller than 13 microns.	Beheng 1987; Aleksić 1989; Ovtchinnikov and Kogan 2000; Phillips et al. 2001; Connolly et al. 2006b; Huang et al. 2008, 2011
Collision fragmentation	Ice–ice collisions produce splinters.	Vardiman 1978, Takahashi et al. 1995	Crystal–crystal collisions Graupel–graupel collisions	Fridlind et al. (2007) Yano and Phillips (2011)
Droplet shattering	Freezing of large droplets produces splinters.	Leisner et al. 2014		Scott and Hobbs 1977; Phillips et al. 2001; Fridlind et al. 2007; Lawson et al. 2015
Sublimation fragmentation	Particles separate from parent ice particle when ice bridge sublimates.	Bacon et al. 1998		

The concept is that accreted supercooled drops release latent heat when they freeze and increase the surface temperature of the ice particle. In contrast, Griggs and Choularton (1986) found that the low temperature cutoff for splinter production is dependent on cloud temperature rather than the surface temperature of the large ice and is unaffected by the accretion rate.

b. Other secondary ice production mechanisms

Secondary ice production by rime splintering (e.g., H-M) is only one of a range of SIP mechanisms or unresolved primary ice formation mechanisms that have been proposed over the last four decades. Many of the hypothesized mechanisms have been associated with evaporative cooling, including fragmentation during evaporation (Schaefer and Cheng 1971; Oraltay and Hallett 1989; Bacon et al. 1998). Other mechanisms involve only the ice phase; for example Vardiman (1978) showed evidence of crystal–crystal collisions leading to fracturing in the laboratory, which has been supported by copious in situ images of fragmented ice in clouds (e.g., Cannon et al. 1974), especially pieces of dendrites. However, there has been little quantification of this mechanism, and observations are compromised by the potential of ice to break on contact

with the aircraft or instruments (e.g., Field et al. 2006). A possible source of crystals that would be involved in this mechanical breakup was identified by Knight (2012), who identified a rapid growth ($2\,\mu m\,s^{-1}$) mode for fine needles at temperatures around −5°C. The thin needle crystals could shatter on impact with other particles (a type of collision fracturing process), providing a source of splinters. This source of fragile needles combined with ice–ice collision fragmentation is a different mechanism from rime splintering but would operate in a similar temperature range. Similarly, graupel–graupel collisions that may occur in convective clouds can also lead to the production of ice splinters (Mizuno and Matsuo 1992; Takahashi et al. 1995).

Although not in-cloud production mechanisms, there are processes that can lead to increased ice concentrations when clouds have been in contact with a snow surface or from blowing snow that is lofted into a cloud layer (Rogers and Vali 1987; Lachlan-Cope et al. 2001; Vali et al. 2012; Lloyd et al. 2015). And there is the possibility that ice can persist in pores of particles even in environmentally subsaturated conditions (Marcolli 2017) that can then grow rapidly larger if the particles are entrained back into more suitable conditions. Both of these effects are due to the reintroduction of ice to cloud rather than the production of new particles.

Splinter production following the freezing of a large millimeter size droplet that subsequently shatters (droplet shattering; e.g., Mason and Maybank 1960; Brownscombe and Thorndike 1968), in contrast to the freezing of a small cloud droplet that impacts a rimer (i.e., rime splintering), is a SIP process that is currently being explored in detail. While Mason and Maybank (1960) found that the splinter production rate decreased with temperature, others have found that this process can operate over a much broader temperature range and may be most efficient between −10° and −15°C (Leisner et al. 2014). As an example of this process, Fig. 7-3 shows high-speed photography of an 80-μm drop producing a spicule and what appears to be secondary ice.

3. In situ observations of SIP

Ice particles are often observed in abundance in convective clouds that are colder than 0°C but with cloud-top temperatures warmer than about −12°C (e.g., Koenig 1963, 1965; Cooper 1986; Hobbs and Rangno 1985; Lawson et al. 2015; Taylor et al. 2016; Ladino et al. 2017). There are also observations to suggest that large ice crystal number concentrations occur in frontal (e.g., Crosier et al. 2011) and supercooled boundary layer stratus cloud (e.g., Rangno and Hobbs 2001). It is commonly reported that crystals

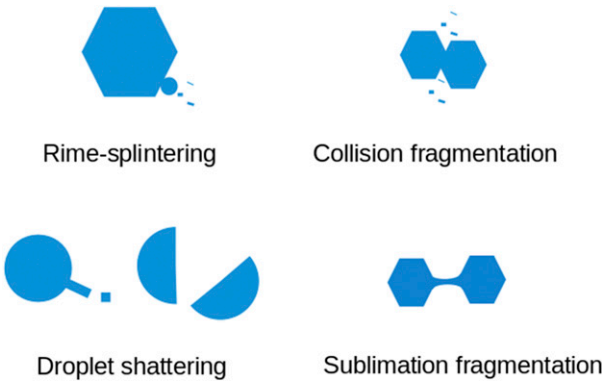

FIG. 7-1. Schematic representation of the SIP outlined in Table 7-1.

thought to be generated by SIP are dominated by needles and columns (see, e.g., Fig. 7-4, showing optical array probe images of cloud particles observed from an aircraft). This particular shape is consistent with the rime splintering process as defined by H-M. These crystals grow in the same temperature range over which Hallett and Mossop found rime splintering to be active in laboratory conditions. These particles would also be consistent with other SIP processes occurring in a similar temperature range, or with formation outside the H-M temperature range followed by subsequent transport into and growth within it.

Notwithstanding instrumentation uncertainties in measurements[1] of both ice crystal concentrations and INPs, measurable concentrations of atmospheric INPs can be smaller by orders of magnitude at these temperatures (DeMott et al. 2010, 2016). For INP concentrations the relatively small sample volumes and background measuring system noise level are challenges that can hinder INP detection at −10°C and warmer temperatures using real-time measuring systems, but steps have been taken to overcome sample volume limitations that impact measurements by making use of large volume air samples collected in flight and then analyzed later for $T > -10$°C (e.g., Lasher-Trapp et al. 2016). Some primary ice nucleation must occur before SIP begins, but the minimum requisite INP number remains uncertain. Despite these uncertainties, there has still been a consistent

[1] See the discussion in Baumgardner et al. (2017, chapter 9) and McFarquhar et al. (2017, chapter 11) about the uncertainties in measurements of the lower-order moments of size distributions, due to shattering of large crystals on probe inlets/tips (chapter 9), small and uncertain sample volumes for small crystals, and uncertainties in algorithms that are designed to remove such concentrations (chapter 11).

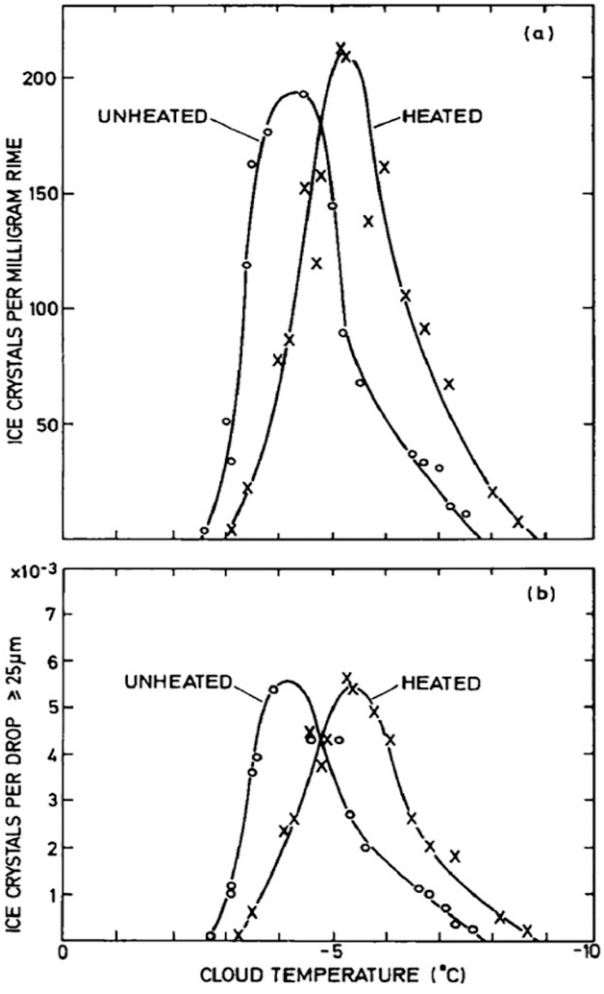

FIG. 7-2. (a) The number of secondary ice crystals produced per milligram of rime accreted upon a metal rod moving at 1.8 m s^{-1}. One curve applies to the case where the rod is electrically heated, the other to the unheated case. (b) As in (a), except that the ordinate represents the number of secondary ice crystals produced per large drop (≥25-μm diameter) accreted. For a point at a given temperature they would be proportionately similar to those in (a). Reproduced from Heymsfield and Mossop (1984).

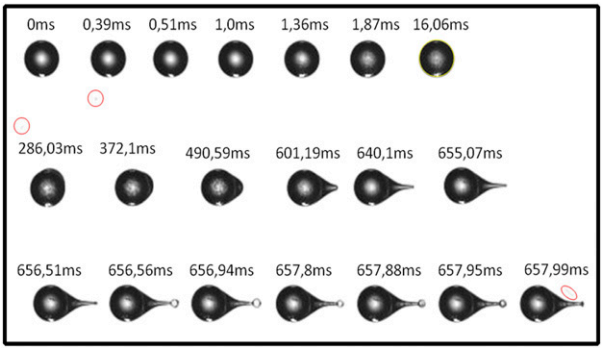

FIG. 7-3. Example of a spicule emitting gas bubbles from an 80-μm diameter suspended drop at −10°C. The red circles identify an ice nucleating particle entering the drop at 0 and 0.39 ms. The red ellipse at 657.99 ms indicates fragments from a burst bubble [adapted with permission from Leisner et al. (2014)].

in situ measurement trend over the past five decades suggesting that a SIP process exists and may explain the difference between INP and ice crystal number concentrations. Nevertheless, reliable quantification of primary ice particle formation is still required to fully constrain SIP.

The discussion in section 2 highlights the variable results from laboratory experiments that have attempted to explain the mechanism of rime-splintering SIP that, along with the production rates, remains uncertain. In situ observations that have attempted to quantify the rate of rime-splintering secondary production have also been fraught with measurement uncertainties. Harris-Hobbs and Cooper (1987) used airborne observations from cumulus clouds in three different geographic regions to estimate secondary ice production rates. This was done by comparing ice size distributions on subsequent passes through the cloud to differences expected by using measured concentrations of droplets and graupel as inputs to the parameterization of Heymsfield and Mossop (1984). Their results are shown in Fig. 7-5. These observations were obtained using probes that would now be regarded as subject to ice crystal shattering (Korolev et al. 2011). In addition, the measurements may be affected by the possibility that ice particles generated by the passage of the aircraft through the cloud (Woodley et al. 2003) from previous cloud passes could have mixed into the measured samples. Considering the potential for relatively large measurement uncertainties, the experiment suggests that the underlying mechanism behaves quantitatively in a way that is broadly comparable with that described by H-M laboratory observations. With improved estimates of the concentrations of particles in the smaller size range the methodology proposed by Harris-Hobbs and Cooper (1987) would likely be better constrained if repeated today.

Hobbs and Rangno (1985, 1990, 1998), in a series of aircraft investigations of maritime cumulus off the coast of Washington, observed relatively high ice concentrations that could not be explained by rime splintering in general and more specifically within the constraints of the H-M mechanism for rime splintering. Their three most salient points are that 1) the clouds glaciated much faster than the laboratory observed H-M splinter rates could explain, 2) the crystal habits observed were often not compatible with the temperature range in which the H-M process operates,

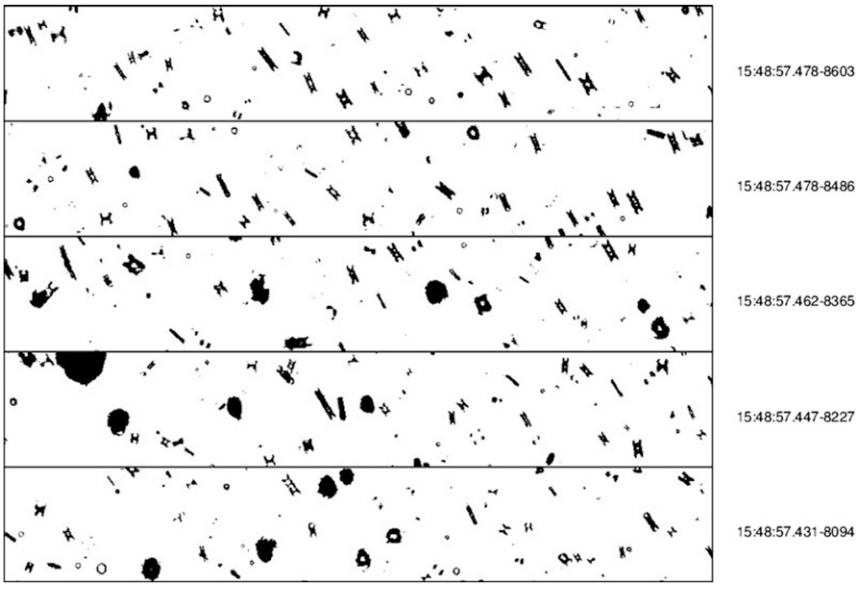

FIG. 7-4. Example 2D-S images of a cloud region where SIP is thought to be active. The width of each horizontal strip is 1280 microns. Visible ice crystal habits are columns (H-shaped particles) and large graupel or frozen droplets. Smaller spherical particles that may be liquid droplets are also visible. Data from a recent flight near Cape Verde at $T = -6$°C, 21 Aug 2015 FAAM BAe146 flight B933.

and 3) high concentrations of small ice particles appeared concurrently with frozen drizzle drops, rather than afterward as would be expected if the smaller crystals were a product of riming–splintering. Possible explanations include transport of splinters out of the rime-splinter zone (e.g., Mason 1998; Blyth and Latham 1997), the importance of other SIP mechanisms (e.g., drop shattering or collision fragmentation during ice–ice collision; (Vardiman 1978; Takahashi et al. 1995; Yano and Phillips 2011; Yano et al. 2016), or a hypothesized primary ice nucleation mechanism not accounted for, such as evaporation ice nucleation (Fridlind et al. 2007).

There have been numerous aircraft observations, some going back more than 50 years, that support the point made by Hobbs and Rangno (1985, 1990, 1998) that high concentrations of ice particles appear concurrently with frozen drizzle drops. Perhaps the most convincing historical data come from observations of tropical maritime cumulus reported by Koenig (1963, 1965). Using impactor data he observed rapid glaciation of tropical cumulus shortly after production of millimeter-diameter supercooled drops in clouds with tops warmer than −12°C. Most recently, similar results were observed by Lawson et al. (2015) and Heymsfield and Willis (2014) in the Caribbean and Africa using state-of-the-art particle imaging probes with shatter-mitigating tips (Lawson et al. 2001, 2006) in cumulus clouds with base temperatures averaging +22°C. Lawson et al. (2015) show a correlation between freezing of millimeter-diameter supercooled drops and production of high ice number concentrations attributed to SIP. Figure 7-6 shows aircraft observations taken within a few hundred meters of cloud top by repeatedly penetrating a rapidly growing convective plume. The imagery (bottom left) at warmer temperatures ($T > -8$°C) and drop size distribution (DSD; bottom right), indicates some millimeter-sized drops among many smaller droplets. On the next pass of the aircraft through the cloud at temperatures between −8° and −12°C some nonspherical particles (assumed to be ice) begin to appear amongst the droplets (middle left) and the ice particles size distribution (PSD) has a low concentration relative to the DSD. The final pass through the cloud at colder temperatures ($T < -12$°C) shows that many different ice habits are present including columns, stellar, and graupel (top left) and that the ice PSD has grown considerably, increasing concentrations from the previous pass by a factor of 10 to 5001^{-1}. Lawson et al. (2015) suggest that the rapid glaciation in these strong updraft cores ($\sim 10\,\mathrm{m\,s^{-1}}$) occurs at temperatures too cold and a rate too fast to be attributable to the H-M process. The authors suggest that the secondary ice particles may have been produced via a droplet shattering process observed in

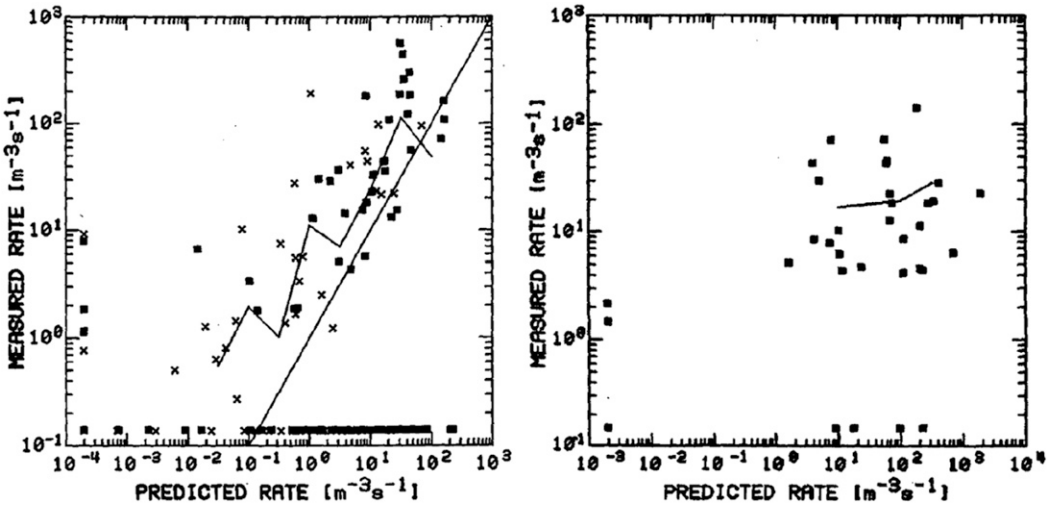

FIG. 7-5. The measured ice crystal production rate as a function of the H-M predicted production rate from (left) California (squares) and Montana measurements (×'s) and (right) Florida measurements. Lines connect the mean observed rates for intervals in the predicted rate, and the straight line in (left) shows 1:1 correspondence between measured and predicted rates [adapted from Harris-Hobbs and Cooper (1987)].

the laboratory (Mason and Maybank 1960; Leisner et al. 2014).

Data on the vertical velocities, liquid water contents (LWCs), and cloud droplet concentrations in the regions where secondary ice particles are formed and observed are needed because they may reflect the process(es) involved. Heymsfield and Willis (2014) found that SIP evidenced by observations of needles–columns throughout the range −3° to −14°C was observed predominantly where the vertical velocities were in the range from −1 to 1 m s^{-1}. The LWCs in the regions where SIP are observed are dominantly below 0.10 g m^{-3}. Median LWCs in these regions were only about 0.03 g m^{-3} with no obvious dependence on the temperature.

Taylor et al. (2016) analyzed aircraft measurements in maritime cumulus with colder (+11°C) cloud-base temperatures that formed over the southwest peninsula of the United Kingdom. They found that almost all of the initial ice particles were frozen drizzle drops [~(0.5–1) mm], whereas vapor-grown ice crystals were dominant in the later stages. Their observations indicate that the freezing of drizzle–raindrops is an important process that dominates the formation of large ice in the intermediate stages of cloud development. In the more mature stage of cloud development the study found high concentrations of small ice within the H-M temperature range. The authors conclude that freezing of large supercooled drops produced via the collision–coalescence and accretion processes is a key to secondary ice production and the timing and location of precipitation. Heymsfield and Willis (2014) found a strong correlation of relatively high concentrations of secondary ice particles in the H-M temperature range in Caribbean and West African maritime tropical cumulus, but only in weak (±2 m s^{-1}) updrafts. They also reported that the first ice particles were large frozen drops. Heymsfield and Willis (2014) hypothesized that locations where there was a balance between updraft velocity and rimer fall speed were favorable for SIP because the time scales for riming would be prolonged and secondary ice splinters would be continuously produced.

It has been speculated that graupel does not need to play the rimer role. In situ observations from frontal cloud systems suggest that riming snowflakes may be able to mediate the SIP (Crosier et al. 2011; Hogan et al. 2002.). However, Stith et al. (2011) found that concentrations of INPs were adequate to explain the observed concentrations of ice in a warm frontal band at temperatures lower than −10°C, when aggregation was taken into account. Thus, for some frontal clouds, SIP is not required to explain the observed ice concentrations.

In Arctic stratus clouds, Rangno and Hobbs (2001) used in situ observations of ice fragments and nonpristine ice to suggest that drop shattering and ice–ice collisional breakup may be important alongside rime splintering to enhance the ice concentrations. The potential importance of drop shattering for SIP is supported by Korolev et al. (2004) and Rangno and Hobbs (2005), who have presented in situ evidence of shattered frozen droplets. The latter, based on the sizes of

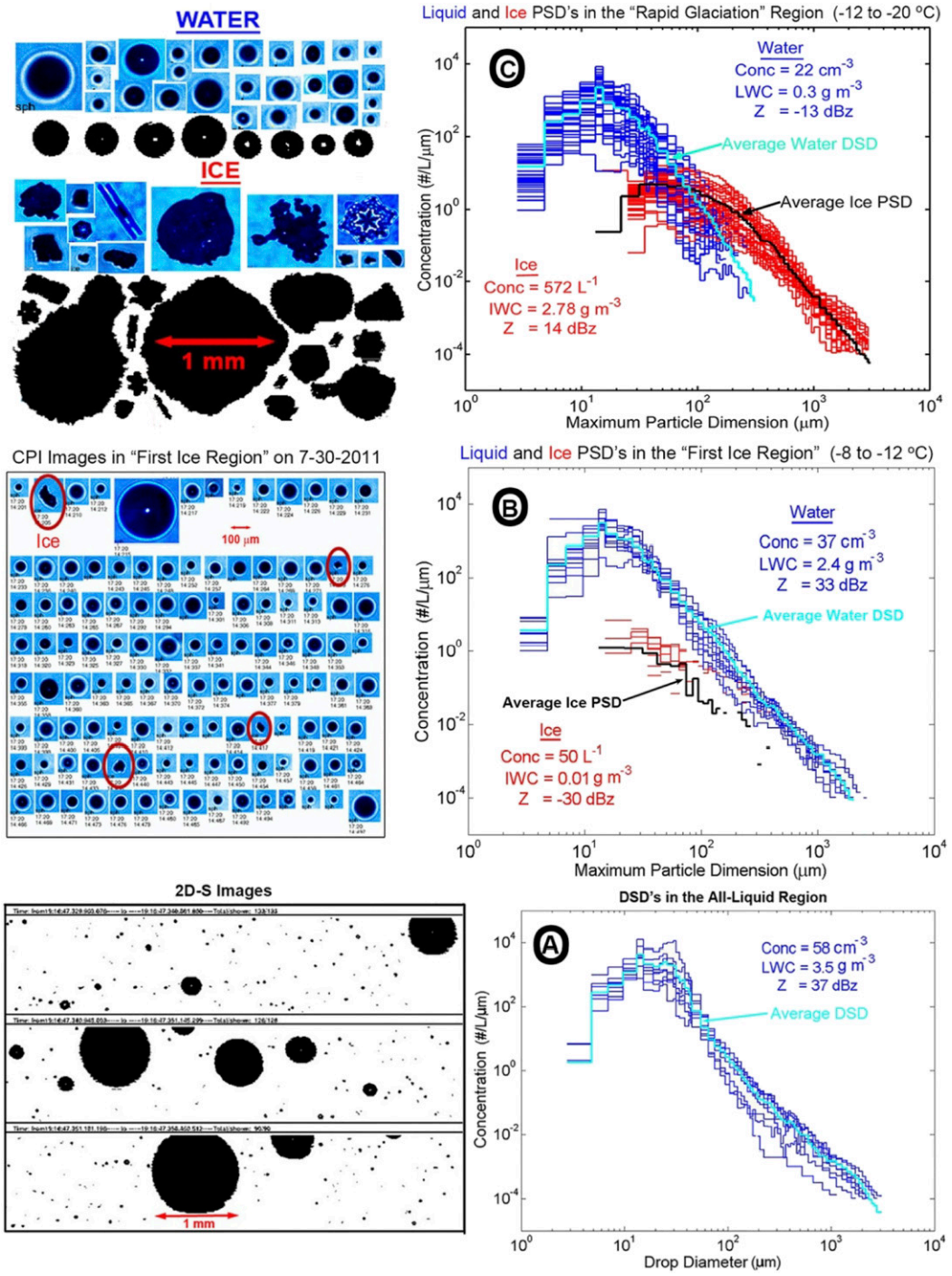

FIG. 7-6. Examples of (left) particle images and (right) size distributions from Learjet penetrations of strong tropical cumulus updraft cores. (bottom right) All penetrations from the all-liquid region ($T > -8$°C), (middle right)) liquid (blue) and ice (red) penetrations from the "first ice" region ($-8° < T < -12$°C), and (top right) penetrations from the "rapid glaciation" region ($-12° < T < -20$°C).

observed fragments, suggests that droplets need to be larger than 50 μm.

Finally, it should be noted that conditions where cloud tops are -12°C and drizzle-sized supercooled droplets are present do not always result in the production of large numbers of ice crystals. Bernstein et al. (2007) and Rasmussen et al. (1995) identified these conditions as long-lived clouds and hazardous for aircraft. If SIP had

been active in these types of shallow layer cloud the supercooled liquid would be rapidly depleted and no longer conducive for aircraft icing.

4. Remote sensing

While aircraft measurements provide a detailed high-resolution view of a small volume of cloud, remote sensing methods probe much larger sample volumes and can provide a much broader volumetric context for observations. However, remote sensing methods that use wavelengths longer than optical wavelengths, such as radar, are less sensitive to small ice crystals than higher-frequency methods. Therefore, dependent upon instrument sensitivity, some cloud evolution needs to occur before particles grow large enough to make a measurable contribution to remotely sensed variables.

Polarimetric radar can provide valuable information on the locations and characteristics of primary and possible secondary ice [see Buehl et al. (2017, chapter 10) for more discussion about the retrieval of cloud properties using radar techniques]. By transmitting horizontally and vertically polarized waves and looking at the differences in power and phase between the echoes in each polarization, information about the orientation and/or phase of the hydrometeors being probed can be obtained, as described below.

In the water saturated conditions where SIP is believed to be most active, ice particles typically grow into pristine geometries dependent upon the temperature at which they grow (e.g., −5°C: columns). These particle shapes have a preferred orientation in the atmosphere, depending on the Reynolds number of the airflow around them, orienting themselves with their longest axis in the horizontal plane. Thus, the magnitude of the backscatter at horizontal polarization is greater than that measured at vertical polarization: the ratio of these two quantities is the differential reflectivity Z_{DR}, typically expressed in dB units. Long solid columns can produce Z_{DR} values of up to 4 dB, while thin plates can produce Z_{DR} as high as 10 dB (e.g., Hogan et al. 2002). Recently, for example, Myagkov et al. (2016) have demonstrated how polarization measurements can be used to detect particle shape and orientation.

Hogan et al. (2002) presented coincident measurements from the Chilbolton Advanced Meteorological Radar (CAMRa) and the Met Office C-130 aircraft, sampling embedded convection in a deep frontal cloud. They observed a region of enhanced Z_{DR} alongside a turret of rising supercooled liquid water droplets (as sampled by the aircraft). Hogan et al. (2002) interpreted this as evidence of columns grown from splinters produced by the H-M rime-splintering process.

TABLE 7-2. Summary of radar signatures useful for probing SIP.

Graupel only	Graupel + splinters	Splinters only
Z_{DR} close to 0dB	Z_{DR} close to 0dB	Z_{DR} up to 4dB
$\rho_{hv} \approx 1$	$\rho_{hv} < 1$	$\rho_{hv} \approx 1$
$K_{DP} \approx 0° \text{km}^{-1}$	$K_{DP} > 0° \text{km}^{-1}$	$K_{DP} > 0° \text{km}^{-1}$
DDV $\approx 0 \text{ m s}^{-1}$	DDV $< 0 \text{ m s}^{-1}$	DDV $\approx 0 \text{ m s}^{-1}$
LDR ≈ -30 dB	LDR ≈ -30 dB	LDR ≈ -15 dB

Crosier et al. (2014) used CAMRa and the Facility for Airborne Atmospheric Measurements (FAAM) aircraft to study the microphysics of line convection in a vigorous cold front. They observed high reflectivity in the updraft core, corresponding to graupel particles, but also observed an inverted U-shaped layer of enhanced Z_{DR} just above it. In situ sampling revealed the particles in this region to be capped columns, and this was interpreted as splinters produced by the H-M rime splintering process transported upward to colder temperatures where platelike features began to grow on the end of the columns.

In both Hogan et al. (2002) and Crosier et al. (2014), high values of Z_{DR} were not observed in the regions where rime splintering was thought to be occurring, but instead were detected as the splinters were lofted by updrafts to another region of the cloud. Graupel particles, thought to be required for the H-M process, are quasi-spherical and have a very small Z_{DR}. But because graupel tend to be large they dominate the radar reflectivity at both polarizations. This means that rime splintering may be associated with high values of Z_{DR}, but only when those splinters are lofted up and separated from the large graupel particles, so that they can be detected.

Just as the backscatter is different for horizontal and vertical polarizations in the presence of oriented ice crystals, so too is the speed at which the radar wave propagates through the cloud. This leads to a small phase shift between the horizontal and vertical polarized echoes, which can be measured by the radar. Since this is a propagation effect, the differential phase shift ϕ_{DP} accumulates as the beam travels through the cloud. By differentiating ϕ_{DP} with range, the one-way specific differential phase shift K_{DP} can be estimated (Kumjian 2013), allowing the location of the oriented crystals in range to be determined. For quasi-spherical particles such as graupel, K_{DP} is close to $0° \text{km}^{-1}$, while for horizontally oriented nonspherical particles a positive K_{DP} is observed as indicated in Table 7-2. Unlike Z_{DR}, K_{DP} has the advantage that it is unaffected by the presence of quasi-spherical graupel or aggregates; however, the data are typically rather noisy because of the small phase difference, and the need to differentiate with range. Nevertheless, Sinclair et al. (2016) show cases where

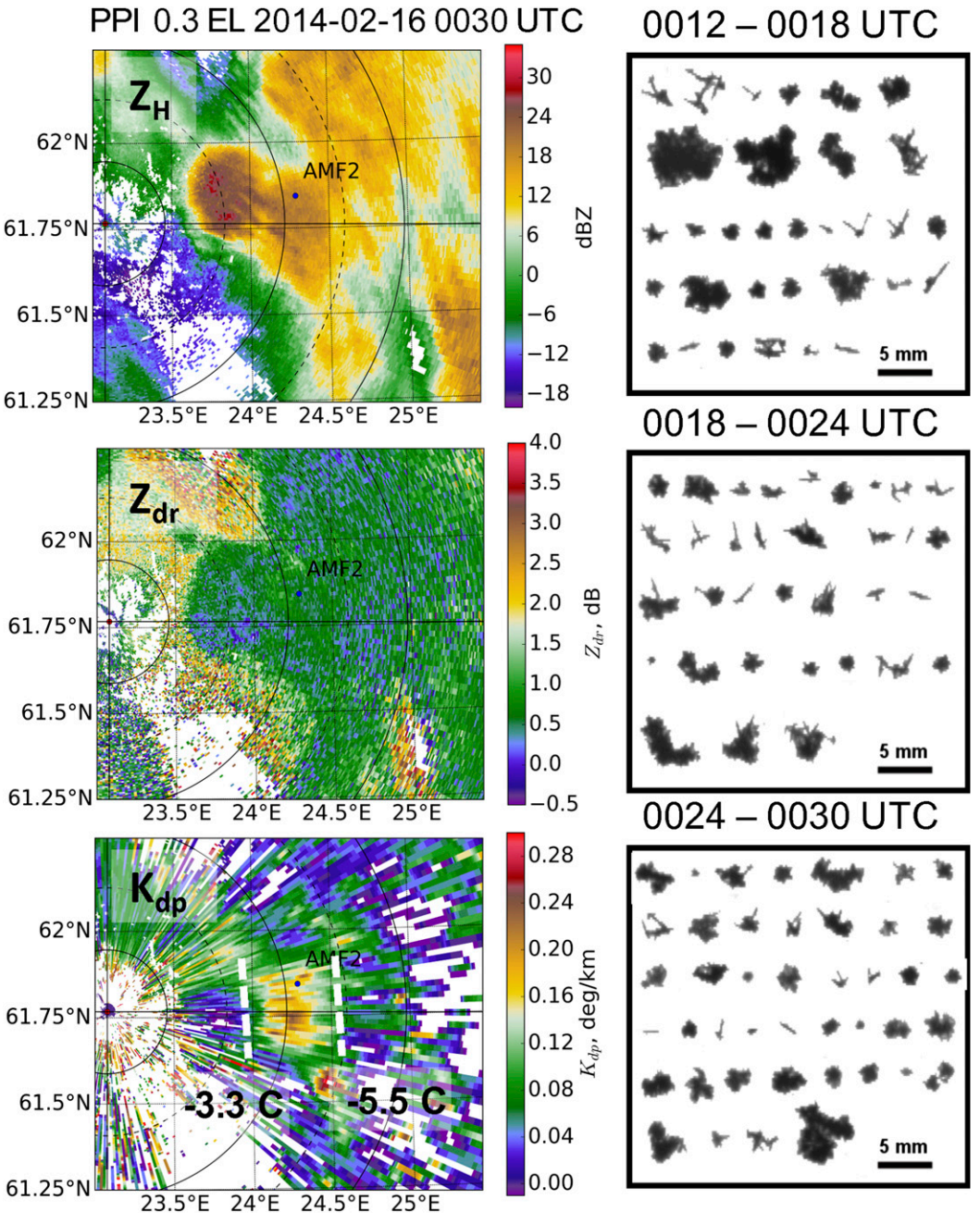

FIG. 7-7. (left top to bottom) Finnish Meteorological Institute Ikaalinen radar plan position indicator observations of equivalent reflectivity Z_H, differential reflectivity $Z_{\rm dr}$, and specific differential phase of a snow storm that took place on 15–16 Feb 2014. The enhanced specific differential phase signature $K_{\rm DP}$, appears in the temperature region between −3° and −5°C. The signature is observed close to the ground and surface precipitation observations indicate presence of columnar crystals, densely rimed particles and aggregates of columnar crystals, as shown in the right column.

bands of high differential phase shift are observed in the H-M temperature range, possibly indicative of new splinter formation Fig. 7-7 shows an example of radar plan position indicator observations (left column) and ice crystal observed at the ground. While the reflectivity (top left) and differential reflectivity (middle left) do not indicate any strong signals, the differential phase shift (bottom right) exhibits a 0.2° $\rm km^{-1}$ signal between −3° and −5°C (the data surface slants upward from the radar located at 61.75°N, 25°E). Since the SIP process can lead

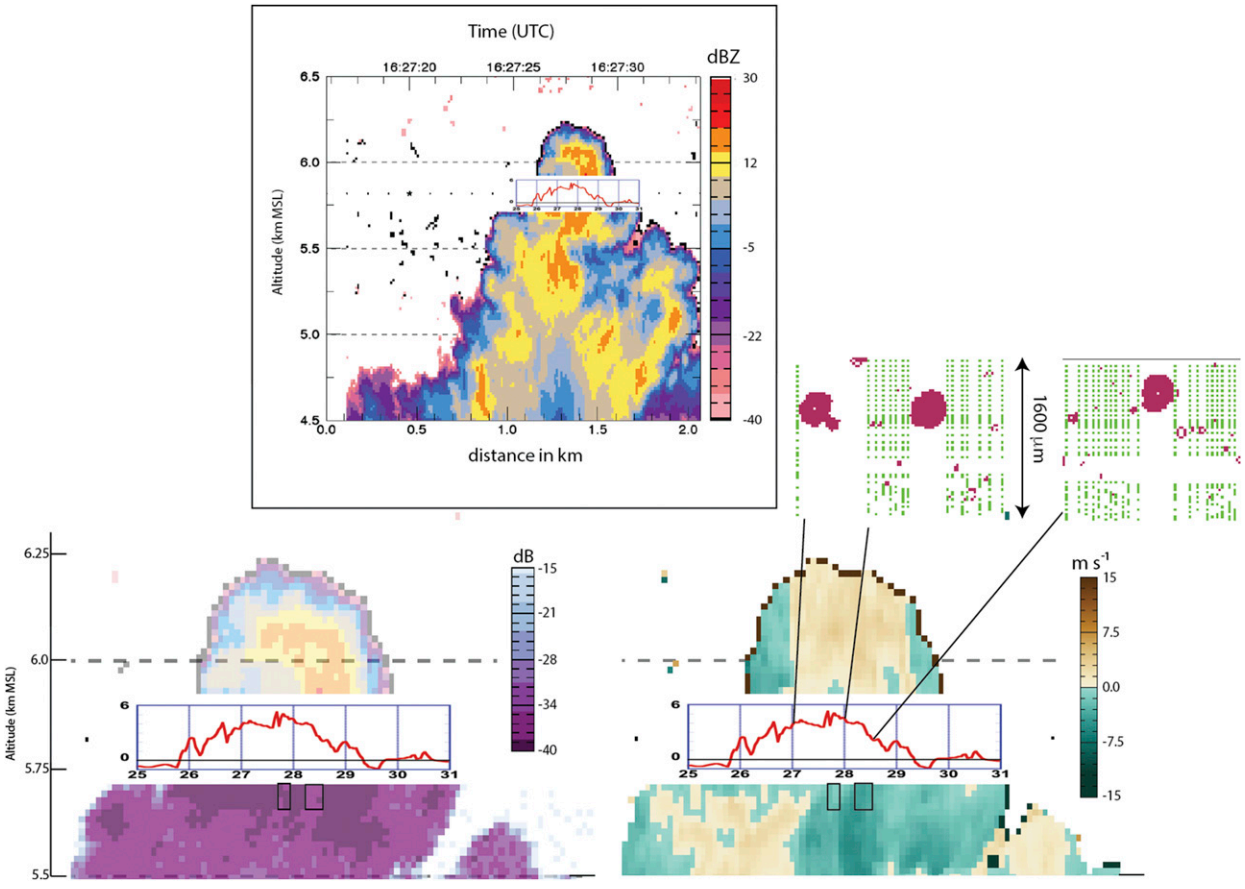

FIG. 7-8. Data from aircraft pass through a convective cloud at −6°C during the ICE-T campaign in the Caribbean, from Lasher-Trapp et al. (2016). (top) Radar reflectivity, (bottom left) LDR and (bottom right) radar derived particle velocities. Examples of graupel images from the 2D-C for the aircraft pass (width of imagery record is 1600 μm) located where shown upon the inset aircraft-measured vertical velocities.

to a mixture of ice particle types (e.g., graupel and splinters) it may be of value to investigate polarization parameters that are sensitive to such mixtures. One such parameter is the copolar correlation coefficient ρ_{hv}. Keat et al. (2015) showed that it is possible to detect mixtures of aggregates and pristine platelike crystals using ρ_{hv}; it seems reasonable therefore to expect that it might also be useful for the detection of rime-splintering situations. Another parameter that is sensitive to shape mixtures is the differential Doppler velocity (DDV; Wilson et al. 1997). If fast-falling quasi-spherical graupel and slow-falling oriented splinters are present in the same volume, a negative value of DDV will be observed.

Lasher-Trapp et al. (2016) analyzed dual-polarization data from an aircraft-mounted W-band radar in tropical cumuli ascending above the 0°C isotherm (see Fig. 7-8). Higher values of the linear depolarization ratio (LDR; indicative of ice) were used to discern graupel traveling through the H-M temperature range, sometimes ascending and descending through it, or even balanced within it, as indicated by the collocated radar-sensed particle velocities. Older and colder clouds were found to contain ribbons of high LDR (~−18 dB), indicative of complete glaciation, where in situ probes (corrected for shattering effects) measured ice particle concentrations exceeding 100 L^{-1}. By combining radar data with in situ particle data corroborating the presence of graupel and supercooled droplets in the H-M temperature range, this study illustrates the ability of in situ polarimetric radars to document the necessary characteristics for a particular SIP in cases where its products cannot be immediately observed.

Radar Doppler spectra profiles also have the potential to detect the results of SIP. Zawadzki et al. (2001) showed examples of a deep frontal cloud where ice particles aloft increased in velocity as they descended to fall at 2–3 m s^{-1}, indicating heavy riming. In the same height interval they observed a second mode in their Doppler spectra, ice particles falling much slower at 0.5 m s^{-1}. This occurred in the −3° to −8°C

temperature range and was interpreted as evidence of the H-M process. Similar observations have been reported by others (e.g., Verlinde et al. 2013; Kalesse et al. 2016). Oue et al. (2015) expanded on this approach by looking at spectra of LDR. They found that their slow-falling crystal population had high LDR (−15 dB) and therefore positively identified them as columns. Thus, the linear depolarization ratio can be used as indicator of ice crystal shape with values for oriented plates being −30 dB or less whereas values for columns can be as high as −15 dB (Matrosov et al. 2001; Bühl et al. 2016).

Table 7-2 summarizes the different polarimetric techniques and typical signature values for identifying hydrometeors. Exploiting synergies and complementarities of different remote sensing techniques like cloud Doppler radars, lidars, and microwave radiometers can help identify conditions that are believed to be needed for SIP, in particular the presence of liquid water. Microwave radiometry can provide estimates of liquid water path in a cloud. Lidar is very sensitive to liquid water clouds, due to the high concentrations of droplets compared to typical ice concentrations in most clouds, and a very distinct spike in backscatter is often a good indicator of the presence of liquid droplets, although high concentrations of ice (such as occur where droplets are freezing homogeneously) can occasionally produce a similar signal. Additionally, lidar linear depolarization ratios (δ) are an indicator of the phase state of the observed hydrometeors, with a high δ indicating nonspherical ice crystals and a δ close to zero indicating spherical liquid-water droplets (Sassen 2005). However, lidar can only penetrate ~3 optical depths into a cloud, and it therefore cannot discern how thick the liquid water cloud is. In contrast, cloud radars are able to penetrate multiple liquid layers and could thus be used to expand the vertically resolved cloud phase identification in the entire vertical column beyond the lidar measurement range, if appropriate algorithms for identifying the liquid layer from radar measurements were developed (e.g., Luke et al. 2010; Bühl et al. 2016).

5. Modeling

a. Representation in models

Modeling studies confirm a significant increase of ice crystal number concentrations due to SIP mechanisms in frontal, cumulus, and some deep convective clouds (e.g., Mason and Maybank 1960; Mossop et al. 1974; Chisnell and Latham 1975, 1976; Koenig and Murray 1977; Aleksić 1989; Phillips et al. 2001; Crawford et al. 2012) Although several SIP mechanisms have been postulated, the most frequently implemented process in numerical models is the H-M rime splintering process (see Table 7-1). Typically, the splinter production rate is related to the number or mass of cloud droplets accreted onto graupel (e.g., Scott and Hobbs 1977; Beheng 1987; Aleksić 1989; Mason 1996; Blyth and Latham 1997; Ovtchinnikov and Kogan 2000; Phillips et al. 2001; Clark et al. 2005; Connolly et al. 2006b; Fridlind et al. 2007; Phillips et al. 2007; Huang et al. 2008; Crawford et al. 2012; Dearden et al. 2016). The splinter production rate is usually assumed to peak at an ambient temperature of −5°C and linearly decreases toward −3° and −8°C (e.g., Cotton et al. 1986). The use of the rimer surface temperature instead of the ambient temperature has been discussed (e.g., Heymsfield and Mossop 1984). Frequently used values for splinter production rates are 1 splinter per 250 accreted drops or 350 splinters per milligram of accreted liquid. In the literature some variation on the assumed temperature thresholds (±0.5°C), the maximum production rates, or application to riming on snow in addition to graupel is found. Based on laboratory findings, some studies compute the riming rate using only drops larger than about 25 μm (e.g., Beheng 1987; Aleksić 1989; Ovtchinnikov and Kogan 2000; Phillips et al. 2001; Connolly et al. 2006b) or requiring the coexistence of droplets larger than 25 μm and smaller than 13 μm (e.g., Huang et al. 2008, 2011). An alternative approach suggested by Harris-Hobbs and Cooper (1987) links the splinter production rate to the fraction of droplets smaller than 13 μm and has been used in several studies (e.g., Geresdi et al. 2005; Sun et al. 2010, 2012). The size, shape, and mass of the ejected splinters are not well constrained from laboratory or observational data. Splinters are typically assumed to be of equal size and their mass is set to the smallest ice crystal mass allowed in the model (e.g., Reisner et al. 1998; Dearden et al. 2016). Several authors have proposed simplified formulations for use in single-moment representations implemented in general circulation models (Bower et al. 1996; Levkov et al. 1992; Storelvmo et al. 2008).

Some attempts have been made to incorporate SIP via other mechanisms (see Table 7-1). Shattering of large supercooled rain drops (e.g., Scott and Hobbs 1977; Phillips et al. 2001; Fridlind et al. 2007; Lawson et al. 2015) has been implemented by prescribing a number of ice crystals emitted from each freezing rain drop that is larger than a threshold diameter (50 to 80 μm). By comparing 1D model simulations with observational data Lawson et al. (2015) suggest a statistical relation between the number of produced splinters and the diameter of the freezing drop. A parameterization of SIP

by crystal–crystal collisions was proposed by Vardiman (1978) but has only been employed by Fridlind et al. (2007). Yano and Phillips (2011) included secondary ice production due to collisions among large (2 mm) graupel, based on laboratory work by Takahashi et al. (1995). Ferrier (1994) has proposed an empirical parameterization for ice enhancement that can be set to act over arbitrary temperature ranges.

b. Sensitivity of simulated cloud physics to SIP

The representation of cloud microphysical processes in general and specifically of (secondary) ice formation in numerical models involves major uncertainties: 1) a priori assumptions regarding the numbers and activity of primary INPs, 2) assumptions made in the representation of hydrometeor size distributions, 3) different formulations of microphysical processes, 4) insufficiently constrained parameters within parameterizations, and 5) insufficient characterization of the atmospheric state from observations. The impact of these uncertainties on modeled clouds and our physical understanding of clouds is often investigated with sensitivity studies where the same case is repeatedly simulated with different models, parameterizations, or initial conditions. However, a better knowledge of the basic physical mechanisms of ice production (both primary and secondary) is required to fully resolve these uncertainties.

The representation of the ice splinter production rate by the rime-splintering H-M process depends upon the rate at which supercooled liquid water is accreted (mass or number depending on model representation). Therefore, the important parameters controlling splinter production rate are the amount of supercooled liquid water and the availability of rimers. The rimers are thought to be generated by the primary ice nucleating particles and hence SIP is intrinsically linked to primary ice formation. Potentially, only very low number concentrations of INPs are needed to initiate SIP. Beard (1992) suggested that primary ice number concentrations of just 10^{-5} to 10^{-3} L^{-1} are sufficient to trigger SIP. Because INP number concentrations control the availability of rimers, decreasing INP number concentration to extremely low values reduces the prevalence of rimers and decreases the efficiency of SIP (Phillips et al. 2007). Increases in INP number concentrations may be expected to enhance splinter production, as was found for deep convective cloud (Connolly et al. 2006b). However, increased number concentrations of primary ice particles can lead to a more efficient Wegner–Bergeron–Findeisen effect that can reduce the supercooled droplet population and inhibit the SIP (Phillips et al. 2003; Clark et al. 2005; Crawford et al. 2012).

Increasing the splinter production rate for the same amount of supercooled liquid accreted was found to decrease the amount of liquid available due to a more effective transfer of liquid to the ice phase (Beheng 1987). Thus, there is potential for a self-limiting feedback whereby greater splinter production rates shorten the time when conditions are conducive to rime splinter production. This perhaps is part of the explanation as to why Connolly et al. (2006b) observed only small impacts of a varying splinter production rate. However, they did find that a doubled splinter production rate increased the cloud-top height and anvil ice content.

If the model representation of rime-splinter production is dependent upon the sizes of droplets accreted, then changes to the drop size distribution through the effects of entrainment (e.g., Phillips et al. 2001), interactions between cloud drops (e.g., Crawford et al. 2012), or aerosol loading (e.g., Scott and Hobbs 1977; Aleksić 1989; Phillips et al. 2001, 2003; Connolly et al. 2006b; Huang et al. 2008) can feed through to the production of ice splinters.

Finally, the treatment of dynamics, mixing, and the microphysics in a model can impact the modeled sensitivity of clouds to SIP processes via their effect on the size distributions and the concentrations of supercooled liquid and rimers (e.g., Aleksić 1989; Phillips et al. 2001; Clark et al. 2005; Phillips et al. 2007; Crawford et al. 2012; Dearden et al. 2016).

c. Model studies using non-rime-splintering SIP

The relative importance of rime splintering and drop shattering was investigated by Chisnell and Latham (1974) with a stochastic parcel model. Drop shattering was found to be important only if splinter production rates due to riming were assumed to be small. In agreement with these results, simulations of Phillips et al. (2001) suggest a significant influence from drop shattering only in the early development stages of cumulus clouds. Parcel model studies focusing on SIP by mechanical fracturing during ice-phase particle collisions suggest a significant ice number concentration enhancements for stratiform clouds with embedded convection, while the impact was small for stratiform and isolated cumulus clouds (Vardiman 1978). The results of Vardiman (1978) further indicated substantial sensitivities to the relative velocity between the colliding particles, the degree of riming, and the width of the size distribution of the involved particles. Theoretical analysis of SIP efficiency by mechanical fracturing for different combinations of ice and small and large graupel particles showed that many mixed-phase clouds fall in the regime for potentially high SIP rates due to mechanical

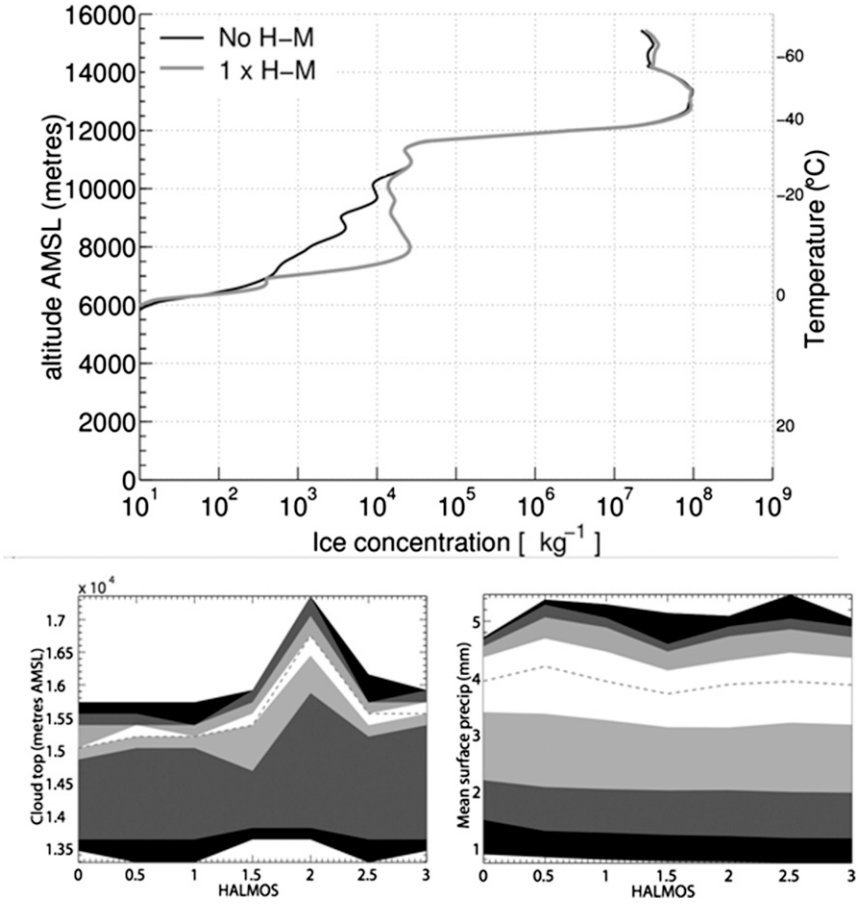

FIG. 7-9. Modeling examples using the Weather Research and Forecasting model showing the impact of SIP on cloud evolution. (top) After Connolly et al. (2006b), the impact of a rime-splintering (H-M) parameterization on ice crystal number mixing ratio. (bottom left) Cloud-top height as a function of H-M (here labeled "HALMOS") splinter production efficiency (1.0 = 1 times standard H-M rate). Shaded contours represent percentiles [gray shadings: 10%–40% and 60%–90% (at 10% intervals)] of domain. (bottom right) Domain mean surface precipitation as a function of H-M splinter production efficiency (from Connolly et al. 2006a).

fracturing (Yano and Phillips 2011; Yano et al. 2016). It was argued that the impact of mechanical fracturing is reduced in clouds with suitable conditions for rime splintering due to the earlier onset of rime splintering based SIP such as H-M (Yano and Phillips 2011). But in cases where conditions are unsuitable for rime splintering, or where the ice from rime splintering does not compete (e.g., due to the lack of sufficient updrafts to carry the SIP to colder temperatures) ice–ice collision produced splintering may be an important mechanism.

d. Importance for weather and climate

The importance of SIP for the larger-scale atmospheric environment can be explored with the aid of numerical models. The validity of such investigations always depends strongly on the realism of the entire numerical model. The few studies conducted thus far indicate minimal impacts on surface precipitation amounts, and rates (e.g., Aleksić 1989; Clark et al. 2005; Connolly et al. 2006a; Crawford et al. 2012; Dearden et al. 2016) except for one case studied by Clark et al. (2005). Clark et al. (2005) suggested that SIP modified the vertical distribution of latent heating in frontal clouds due to altered vapor deposition and sublimation rates. However, Dearden et al. (2016) found no significant impact of SIP on latent heating in a bent back frontal cloud case. Several studies have assessed the influence of SIP on cloud electrification and lightning (e.g., Baker et al. 1995, 1999; Latham et al. 2004; Mansell et al. 2010; Mansell and Ziegler 2013).

Connolly et al. (2006a) have shown that the maximum vertical velocity, the cloud-top height (Fig. 7-9), and the anvil ice water content of a deep convective storm were sensitive to enhanced splinter production rates leading to a net radiative forcing of 10 W m^{-2}. The lack of explicit treatment of SIP in convective parameterizations potentially has implications for climate modeling, where cloud-top height is important for water distribution in the troposphere and transfer into the stratosphere (Hardiman et al. 2015) and characteristics of the anvil affect the atmospheric radiative balance.

6. Discussion and conclusions

It is clear that the thousand-fold or more amplification of observed ice crystal number concentrations above those of natural INP concentrations mean that SIP is an important process for cloud evolution. SIP has been detected in the natural clouds, reproduced under laboratory conditions, and implemented in cloud models. However, there is no consensus on the physical mechanism(s) of most importance under particular atmospheric conditions. Rates of splinter production are not well constrained, nor is there a complete understanding of how these rates vary with changing environmental or cloud characteristics.

Despite the many uncertainties about the role of SIP in frontal clouds and mixed-phase low level stratus clouds, observations from natural convective clouds tend to exhibit a repeatable pattern. Convective clouds that have relatively warm bases (i.e., $T > \sim +10$°C) with a broad drop distribution just above cloud base have a strong tendency to form raindrops (e.g., Lawson et al. 2015). Similar clouds but with a greater cloud-base temperatures ($T > \sim +15$°C) are likely to produce even more raindrops and some may ascend above the freezing level if the updraft is strong and deep enough (e.g., Hallett et al. 1978). It has been suggested by, for example, Koenig (1963) and Lawson et al. (2015) that supercooled raindrops play an important role in the initiation of the glaciation process and there is evidence that this can occur at temperatures greater than −10°C.

The concentration of ice formed through primary ice nucleation, the initial nucleation mechanism, and the minimum concentration of INPs required to initiate SIP in these clouds is not known or understood. There are some suggestions that the SIP that occurs after the coalescence process generates supercooled raindrops may take place too rapidly to be generated via H-M (Lawson et al. 2015).

Supercooled raindrops are most often observed to occur in tropical maritime clouds. However, they have also been observed in midlatitude maritime (e.g., Huang et al. 2008; Taylor et al. 2016) and continental clouds (e.g., Blyth and Latham 1993) although their occurrence is rarer (e.g., Cannon et al. 1974). Following the initial freezing of supercooled raindrops a rapid glaciation of the cloud is usually observed. The mechanism, rates, and dependence of environmental conditions are again subject to uncertainty.

There is agreement on the following points:

- Measured ice particle number concentrations have been observed to exceed estimates of primary ice nucleation particle concentrations by 1 to 3 orders of magnitude
- The onset of the rapid glaciation of convective clouds is observed to occur shortly after millimeter-size drops freeze.
- Polarimetric radar signatures are coincident with regions where aircraft observations suggest that SIP has been active recently
- Modeling is dominated by one representation of SIP (H-M) and results of the impact of SIP on precipitation appear small but cloud evolution varies from case to case and model to model.

Looking forward there is a need to understand and better constrain SIP in the laboratory, in the atmosphere, and in its representation in models. The following questions and recommendations are posed to help frame and motivate future research.

Outstanding secondary ice production questions include the following:

- *What is the dominant secondary ice production mechanism in the atmosphere?* Is it any of those identified in the laboratory? How applicable are laboratory experiments to clouds in the atmosphere?
- *How prevalent is secondary ice production in the atmosphere?* In which types of clouds is the process active, and is the process important for NWP and climate modeling? Operational radar networks across Europe and America are being upgraded to dual-polarization, leading to a wealth of currently untapped statistical information on the occurrence of SIP, and their role in precipitation development.
- *Why is it often observed that large (>1 mm) drops are needed for SIP?* Is it to accumulate sufficient aerosol for a freezing event to take place at warm (−5°C) temperatures? Is there one type of INP that is responsible for first ice at these temperatures, or will a wide range of different types of INPs satisfy? Does recirculation of INPs or small ice play a role?
- *What is the minimum INP concentration required to initiate SIP?* Under what conditions will these

concentrations apply? Some initial primary ice formation is required before SIP can begin.

The following recommendations are made:

- *Improve capabilities for measuring INP concentrations at modest supercooling ($T > -10°C$)*, especially in real-time systems. This is required to determine what INP concentrations are required to start SIP.
- *Improve the representation of INPs in models to include actual concentrations and activities of INPs.* Improve sensitivity studies of SIP and understand in which regimes SIP will be most important.
- *Extend testing of rime splintering (traditional H-M) and other SIP processes in the laboratory.* More accurate measurements and better constraints on splinter production rates and characterization of the splinter population for varying parameters are required.
- *Improve experimental field observations to confirm proposed physical mechanisms of splinter production.* Without detailed knowledge of the important physical mechanisms that control splinter production, modeling SIP and the evolution of cloud and cloud fields will be highly uncertain. The combination of in situ measurements from aircraft and dual polarized Doppler radar is a powerful approach.
- *Improve instruments for measuring ice in clouds.* One of the major impediments to our understanding of ice formation is the difficulty of gathering experimental evidence for ice formation, especially in mixed phase clouds. Improvements in the measurement of the size, shape, and number concentrations of ice particles in the sub-150-μm size range are required.
- *Carry out integrated field programs involving in situ sampling, remote sensing, and modeling studies.* Quantitative comparisons between model output and observations, both by forward modeling of the model microphysical fields to generate radar dual polarization parameters and through retrievals, are required to test models. Remote sensing techniques also raise the possibility of studying the evolution of the secondary ice particles after they have formed, while aircraft sampling allows high-resolution snapshots and provides important information for constraining the remote sensing. A number of aircraft sampling strategies, including multiple aircraft, may be needed to utilize the recent capabilities of improved remote sensing and in situ measurement capabilities to answer remaining questions surrounding SIP. Targeting specific types of clouds that allow for isolating physical mechanisms for testing are likely candidates for future experiments. For example, sampling strategies have recently focused on ''chimney clouds'' (so called because of their aspect ratio) with no observable anvil remnants above. These fresh turrets exhibit large vertical velocities ($>10\,m\,s^{-1}$). By following the tops of these turrets up it is possible to observe the evolution from liquid to fully glaciated cloud, with less contamination from older cloud regions. These clouds could be compared with observations in upslope supercooled layer clouds where cloud-top temperatures can be warmer than $-12°C$ and supercooled drizzle drops are present, but SIP may not be occurring.
- *Carry out model intercomparison studies.* This would quantify the sensitivity of SIP to parametric uncertainty across a range of models with different microphysical representations from climate model configurations to detailed bin model representations.

Acknowledgments. We wish to memorialize this chapter to Paul Willis, whose tireless measurements in ice clouds led to new insight into where and when secondary particles are observed. The authors would like to thank the many sponsors who have provided funding for the monograph: Leibniz Institute for Tropospheric Research (TROPOS), Forschungszentrum Jülich (FZJ), and Deutsches Zentrum für Luft- und Raumfahrt (DLR), Germany; ETH Zurich, Switzerland; National Center for Atmospheric Research (NCAR), United States; the Met Office, United Kingdom; the University of Illinois, United States; Environment and Climate Change Canada (ECCC), Canada; National Science Foundation (NSF), AGS 1723548, National Aeronautics and Space Administration (NASA), United States; the International Commission on Clouds and Precipitation (ICCP), the European Facility for Airborne Research (EUFAR), and Droplet Measurement Technologies (DMT), United States. NCAR is sponsored by the NSF. Any opinions, findings, and conclusions or recommendations expressed in this publication are those of the author(s) and do not necessarily reflect the views of the National Science Foundation.

REFERENCES

Aleksić, N., 1989: Precipitation effects of hail suppression in Serbia. *Theor. Appl. Climatol.*, **40**, 271–279, doi:10.1007/BF00865978.

Bacon, N. J., B. D. Swanson, M. B. Baker, and E. J. Davis, 1998: Breakup of levitated frost particles. *J. Geophys. Res.*, **103**, 13 763–13 775, doi:10.1029/98JD01162.

Baker, M. B., H. J. Christian, and J. Latham, 1995: A computational study of the relationships linking lightning frequency and other thundercloud parameters. *Quart. J. Roy. Meteor. Soc.*, **121**, 1525–1548, doi:10.1002/qj.49712152703.

——, A. M. Blyth, H. J. Christian, J. Latham, K. L. Miller, and A. M. Gadian, 1999: Relationships between lightning activity and various thundercloud parameters: Satellite and modelling studies. *Atmos. Res.*, **51**, 221–236, doi:10.1016/S0169-8095(99)00009-5.

Baumgardner, D., and Coauthors, 2017: In situ measurement challenges. *Ice Formation and Evolution in Clouds and Precipitation: Measurement and Modeling Challenges*, *Meteor. Monogr.*, No. 58, Amer. Meteor. Soc., doi:10.1175/AMSMONOGRAPHS-D-16-0011.1.

Beard, K. V., 1992: Ice initiation in warm-base convective clouds. An assessment of microphysical mechanisms. *Atmos. Res.*, **28**, 125–152, doi:10.1016/0169-8095(92)90024-5.

Beheng, K. D., 1987: Microphysical properties of glaciating cumulus clouds: Comparison of measurements with a numerical simulation. *Quart. J. Roy. Meteor. Soc.*, **113**, 1377–1382, doi:10.1002/qj.49711347815.

Bernstein, B., C. Wolff, and F. McDonought, 2007: An inferred climatology of icing conditions aloft, including supercooled large drops. Part I: Canada and the continental United States. *J. Appl. Meteor. Climatol.*, **46**, 1857–1878, doi:10.1175/2007JAMC1607.1.

Blyth, A. M., and J. Latham, 1993: Development of ice and precipitation in New Mexican summertime cumulus clouds. *Quart. J. Roy. Meteor. Soc.*, **119**, 91–120, doi:10.1002/qj.49711950905.

——, and ——, 1997: A multi-thermal model of cumulus glaciation via the Hallett-Mossop process. *Quart. J. Roy. Meteor. Soc.*, **123**, 1185–1198, doi:10.1002/qj.49712354104.

Bower, K. N., S. J. Moss, D. W. Johnson, T. W. Choularton, J. Latham, P. R. A. Brown, A. M. Blyth, and J. Cardwell, 1996: A parameterization of the ice water content observed in frontal and convective clouds. *Quart. J. Roy. Meteor. Soc.*, **122**, 1815–1844, doi:10.1002/qj.49712253605.

Brewer, A. W., and H. P. Palmer, 1949: Condensation processes at low temperatures, and the production of new sublimation nuclei by the splintering of ice. *Nature*, **164**, 312–313, doi:10.1038/164312a0.

Brownscombe, J. L., and N. S. C. Thorndike, 1968: Freezing and shattering of water droplets in freefall. *Nature*, **220**, 687–689, doi:10.1038/220687a0.

Buehl, J., and Coauthors, 2017: Remote sensing. *Ice Formation and Evolution in Clouds and Precipitation: Measurement and Modeling Challenges*, *Meteor. Monogr.*, No. 58, Amer. Meteor. Soc., doi:10.1175/AMSMONOGRAPHS-D-16-0015.1.

Bühl, J., P. Seifert, A. Myagkov, and A. Ansmann, 2016: Measuring ice- and liquid-water properties in mixed-phase cloud layers at the Leipzig Cloudnet station. *Atmos. Chem. Phys.*, **16**, 10 609–10 620, doi:10.5194/acp-16-10609-2016.

Cannon, T. W., J. E. Dye, and V. Toutenhoofd, 1974: The mechanism of precipitation formation in northeastern Colorado cumulus II. Sailplane measurements. *J. Atmos. Sci.*, **31**, 2148–2151, doi:10.1175/1520-0469(1974)031<2148:TMOPFI>2.0.CO;2.

Cantrell, W., and A. Heymsfield, 2005: Production of ice in tropospheric clouds: A review. *Bull. Amer. Meteor. Soc.*, **86**, 795–807, doi:10.1175/BAMS-86-6-795.

Chisnell, R. F., and J. Latham, 1974: A stochastic model of ice particle multiplication by drop splintering. *Quart. J. Roy. Meteor. Soc.*, **100**, 296–308, doi:10.1002/qj.49710042504.

——, and ——, 1975: Multiplication of ice particles in slightly supercooled cumulus. *J. Atmos. Sci.*, **32**, 863–866, doi:10.1175/1520-0469(1975)032<0863:MOIPIS>2.0.CO;2.

——, and ——, 1976: Ice particle multiplication in cumulus clouds. *Quart. J. Roy. Meteor. Soc.*, **102**, 133–156, doi:10.1002/qj.49710243111.

Choularton, T. W., D. J. Griggs, B. Y. Humood, and J. Latham, 1980: Laboratory studies of riming, and its relation to ice splinter production. *Quart. J. Roy. Meteor. Soc.*, **106**, 367–374, doi:10.1002/qj.49710644809.

Clark, P., T. W. Choularton, P. R. A. Brown, P. R. Field, A. J. Illingworth, and R. J. Hogan, 2005: Numerical modelling of mixed-phase frontal clouds observed during the CWVC project. *Quart. J. Roy. Meteor. Soc.*, **131**, 1677–1693, doi:10.1256/qj.03.210.

Connolly, P. J., T. W. Choularton, M. W. Gallagher, K. N. Bower, M. J. Flynn, and J. A. Whiteway, 2006a: Cloud-resolving simulations of intense tropical *Hector* thunderstorms: Implications for aerosol–cloud interactions. *Quart. J. Roy. Meteor. Soc.*, **132**, 3079–3106, doi:10.1256/qj.05.86.

——, A. J. Heymsfield, and T. W. Choularton, 2006b: Modelling the influence of rimer surface temperature on the glaciation of intense thunderstorms: The rime–splinter mechanism of ice multiplication. *Quart. J. Roy. Meteor. Soc.*, **132**, 3059–3077, doi:10.1256/qj.05.45.

Cooper, W. A., 1986: Ice initiation in nature clouds. *Precipitation Enhancement—A Scientific Challenge*, *Meteor. Monogr.*, No. 43, Amer. Meteor. Soc., 29–32.

Cotton, W. R., G. J. Tripoli, R. Rauber, and E. Mulvihill, 1986: Numerical simulation of the effects of varying ice crystal nucleation rates and aggregation processes on orographic snowfall. *J. Climate Appl. Meteor.*, **25**, 1658–1680, doi:10.1175/1520-0450(1986)025<1658:NSOTEO>2.0.CO;2.

Crawford, I., and Coauthors, 2012: Ice formation and development in aged, wintertime cumulus over the UK: Observations and modelling. *Atmos. Chem. Phys.*, **12**, 4963–4985, doi:10.5194/acp-12-4963-2012.

Crosier, J., and Coauthors, 2011: Observations of ice multiplication in a weakly convective cell embedded in supercooled mid-level stratus. *Atmos. Chem. Phys.*, **11**, 257–273, doi:10.5194/acp-11-257-2011.

——, and Coauthors, 2014: Microphysical properties of cold frontal rainbands. *Quart. J. Roy. Meteor. Soc.*, **140**, 1257–1268, doi:10.1002/qj.2206.

Dearden, C., G. Vaughan, T. Tsai, and J. Chen, 2016: Exploring the diabatic role of ice microphysical processes in two North Atlantic summer cyclones. *Mon. Wea. Rev.*, **144**, 1249–1272, doi:10.1175/MWR-D-15-0253.1.

DeMott, P. J., and Coauthors, 2010: Predicting global atmospheric ice nuclei distributions and their impacts on climate. *Proc. Natl. Acad. Sci. USA*, **107**, 11 217–11 222, doi:10.1073/pnas.0910818107.

——, and Coauthors, 2011: Resurgence in ice nuclei measurement research. *Bull. Amer. Meteor. Soc.*, **92**, 1623–1635, doi:10.1175/2011BAMS3119.1.

——, and Coauthors, 2016: Sea spray aerosol as a unique source of ice nucleating particles. *Proc. Natl. Acad. Sci. USA*, 113, 5797–5803, doi:10.1073/pnas.1514034112.

Dong, Y. Y., and J. Hallett, 1989: Droplet accretion during rime growth and the formation of secondary ice crystals. *Quart. J. Roy. Meteor. Soc.*, **115**, 127–142, doi:10.1002/qj.49711548507.

Ferrier, B. S., 1994: A double-moment multiple-phase four-class bulk ice scheme. Part I: Description. *J. Atmos. Sci.*, **51**, 249–280, doi:10.1175/1520-0469(1994)051<0249:ADMMPF>2.0.CO;2.

Field, P. R., A. J. Heymsfield, and A. Bansemer, 2006: Shattering and particle interarrival times measured by optical array probes in ice clouds. *J. Atmos. Oceanic Technol.*, **23**, 1357–1371, doi:10.1175/JTECH1922.1.

Findeisen, W., and E. Findeisen, 1943: Untersuchungen uber die Eissplitterbildung an Reifschichten (Ein Beitrag zur Frage der Entstehung der Gewitterelektrizitat und zur Mikrostruktur der Cumulonimben). *Meteor. Z.*, **60**, 145–154.

Fridlind, A. M., A. S. Ackerman, G. McFarquhar, G. Zhang, M. R. Poellot, P. J. DeMott, A. J. Prenni, and A. J. Heymsfield, 2007: Ice properties of single-layer stratocumulus during the Mixed-Phase Arctic Cloud Experiment: 2. Model results. *J. Geophys. Res.*, **112**, D24202, doi:10.1029/2007JD008646.

Geresdi, I., R. Rasmussen, W. Grabowski, and B. Bernstein, 2005: Sensitivity of freezing drizzle formation in stably stratified clouds to ice processes. *Meteor. Atmos. Phys.*, **88**, 91–105, doi:10.1007/s00703-003-0048-5.

Griggs, D. J., and T. W. Choularton, 1983: Freezing modes of riming droplets with application to ice splinter production. *Quart. J. Roy. Meteor. Soc.*, **109**, 243–253, doi:10.1002/qj.49710945912.

——, and ——, 1986: The effect of rimer surface temperature on ice splinter production by the Hallett-Mossop process. *Quart. J. Roy. Meteor. Soc.*, **112**, 1254–1256, doi:10.1002/qj.49711247419.

Hallett, J., and S. C. Mossop, 1974: Production of secondary ice particles during the riming process. *Nature*, **249**, 26–28, doi:10.1038/249026a0.

——, R. I. Sax, D. Lamb, and A. S. R. Murty, 1978: Aircraft measurements of ice in Florida cumuli. *Quart. J. Roy. Meteor. Soc.*, **104**, 631–651, doi:10.1002/qj.49710444108.

Hardiman, S. C., and Coauthors, 2015: Processes controlling tropical tropopause temperature and stratospheric water vapor in climate models. *J. Climate*, **28**, 6516–6535, doi:10.1175/JCLI-D-15-0075.1.

Harris-Hobbs, R. L., and W. A. Cooper, 1987: Field evidence supporting quantitative predictions of secondary ice production rates. *J. Atmos. Sci.*, **44**, 1071–1082, doi:10.1175/1520-0469(1987)044<1071:FESQPO>2.0.CO;2.

Heymsfield, A. J., and S. C. Mossop, 1984: Temperature dependence of secondary ice crystal production during soft hail growth by riming. *Quart. J. Roy. Meteor. Soc.*, **110**, 765–770, doi:10.1002/qj.49711046512.

——, and P. Willis, 2014: Cloud conditions favoring secondary ice particle production in tropical maritime convection. *J. Atmos. Sci.*, **71**, 4500–4526, doi:10.1175/JAS-D-14-0093.1.

Hobbs, P. V., and A. L. Rangno, 1985: Ice particle concentrations in clouds. *J. Atmos. Sci.*, **42**, 2523–2549, doi:10.1175/1520-0469(1985)042<2523:IPCIC>2.0.CO;2.

——, and ——, 1990: Rapid development of high ice particle concentrations in small polar maritime cumuliform clouds. *J. Atmos. Sci.*, **47**, 2710–2722, doi:10.1175/1520-0469(1990)047<2710:RDOHIP>2.0.CO;2.

——, and ——, 1998: Microstructures of low and middle-level clouds over the Beaufort Sea. *Quart. J. Roy. Meteor. Soc.*, **124**, 2035–2071, doi:10.1002/qj.49712455012.

Hogan, R. J., P. R. Field, A. J. Illingworth, R. J. Cotton, and T. W. Choularton, 2002: Properties of embedded convection in warm-frontal mixed-phase cloud from aircraft and polarimetric radar. *Quart. J. Roy. Meteor. Soc.*, **128**, 451–476, doi:10.1256/003590002321042054.

Huang, Y., and Coauthors, 2011: Development of ice particles in convective clouds observed over the black forest mountains during COPS. *Quart. J. Roy. Meteor. Soc.*, **137**, 275–286, doi:10.1002/qj.749.

——, and Coauthors, 2008: The development of ice in a cumulus cloud over southwest England. *New J. Phys.*, **10**, 105021, doi:10.1088/1367-2630/10/10/105021.

Kalesse, H., W. Szyrmer, S. Kneifel, P. Kollias, and E. Luke, 2016: Fingerprints of a riming event on cloud radar Doppler spectra: Observations and modelling. *Atmos. Chem. Phys.*, **16**, 2997–3012, doi:10.5194/acp-16-2997-2016.

Keat, W. J., C. Westbrook, and A. Illingworth, 2015: Retrieving the microphysics of mixed-phase regions embedded within deep ice clouds using dual polarisation radar. *37th Conf. on Radar Meteorology*, Norman, OK, Amer. Meteor. Soc., 1A.6. [Available online at https://ams.confex.com/ams/37RADAR/webprogram/Paper275777.html.]

Knight, C. A., 2012: Ice growth from the vapor at −5°C. *J. Atmos. Sci.*, **69**, 2031–2040, doi:10.1175/JAS-D-11-0287.1.

Koenig, L. R., 1963: The glaciating behavior of small cumulonimbus clouds. *J. Atmos. Sci.*, **20**, 29–47, doi:10.1175/1520-0469(1963)020<0029:TGBOSC>2.0.CO;2.

——, 1965: Drop freezing through drop breakup. *J. Atmos. Sci.*, **22**, 448–451, doi:10.1175/1520-0469(1965)022<0448:DFTDB>2.0.CO;2.

——, and F. W. Murray, 1977: The rime-splintering hypothesis of cumulus glaciation examined using a field-of-flow cloud model. *Quart. J. Roy. Meteor. Soc.*, **103**, 585–606, doi:10.1002/qj.49710343805.

Korolev, A. V., E. Emery, J. Strapp, S. Cober, G. Isaac, M. Wasey, and D. Marcotte, 2011: Small ice particles in tropospheric clouds: Fact or artifact? Airborne Icing Instrumentation Evaluation Experiment. *Bull. Amer. Meteor. Soc.*, **92**, 967–973, doi:10.1175/2010BAMS3141.1.

——, M. P. Bailey, J. Hallett, and G. A. Isaac, 2004: Laboratory and in-situ observation of deposition growth of frozen drops. *J. Appl. Meteor.*, **43**, 612–622, doi:10.1175/1520-0450(2004)043<0612:LAISOO>2.0.CO;2.

Kumjian, M. R., 2013: Principles and applications of dual-polarization weather radar. Part I: Description of the polarimetric radar variables. *J. Oper. Meteor.*, **1**, 226–242, doi:10.15191/nwajom.2013.0119.

Lachlan-Cope, T., R. Ladkin, J. Turner, and P. Davison, 2001: Observations of cloud and precipitation particles on the Avery Plateau, Antarctic Peninsula. *Antarct. Sci.*, **13**, 339–348, doi:10.1017/S0954102001000475.

Ladino, L. A., A. Korolev, I. Heckman, M. Wolde, A. M. Fridlind, and A. S. Ackerman, 2017: On the role of ice-nucleating aerosol in the formation of ice particles in tropical mesoscale convective systems. *Geophys. Res. Lett.*, **44**, 1574–1582, doi:10.1002/2016GL072455.

Lasher-Trapp, S., D. C. Leon, P. J. DeMott, C. M. Villanueva-Birriel, A. V. Johnson, D. H. Moser, C. S. Tully, and W. Wu, 2016: A multisensor investigation of rime splintering in tropical maritime cumuli. *J. Atmos. Sci.*, **73**, 2547–2564, doi:10.1175/JAS-D-15-0285.1.

Latham, J., A. M. Blyth, H. J. Christian Jr., W. Deierling, and A. M. Gadian, 2004: Determination of precipitation rates and yields from lightning measurements. *J. Hydrol.*, **288**, 13–19, doi:10.1016/j.jhydrol.2003.11.009.

Lawson, R. P., B. A. Baker, C. G. Schmitt, and T. L. Jensen, 2001: An overview of microphysical properties of Arctic clouds observed in May and July 1998 during FIRE ACE. *J. Geophys. Res.*, **106**, 14 989–15 014, doi:10.1029/2000JD900789.

——, D. O'Connor, P. Zmarzly, K. Weaver, B. Baker, Q. Mo, and H. Jonsson, 2006: The 2D-S (Stereo) probe: Design and preliminary tests of a new airborne, high-speed, high-resolution particle Imaging probe. *J. Atmos. Oceanic Technol.*, **23**, 1462–1477, doi:10.1175/JTECH1927.1.

——, S. Woods, and H. Morrison, 2015: The microphysics of ice and precipitation development in tropical cumulus clouds. *J. Atmos. Sci.*, **72**, 2429–2445, doi:10.1175/JAS-D-14-0274.1.

Leisner, T., T. Pander, P. Handmann, and A. Kiselev, 2014: Secondary ice processes upon heterogeneous freezing of cloud droplets. *14th Conf. on Cloud Physics and Atmospheric Radiation*, Boston, MA, Amer. Meteor. Soc., 2.3. [Available online at https://ams.confex.com/ams/14CLOUD14ATRAD/webprogram/Paper250221.html.]

Levkov, L. B., B. Rockel, H. Kapitza, and E. Raschke, 1992: 3D mesoscale numerical studies of cirrus and stratus clouds by their time and space evolution. *Beitr. Phys. Atmos.*, **65**, 35–58.

Lloyd, G., and Coauthors, 2015: The origins of ice crystals measured in mixed-phase clouds at the high-alpine site Jungfraujoch. *Atmos. Chem. Phys.*, **15**, 12 953–12 969, doi:10.5194/acp-15-12953-2015.

Luke, E., and Coauthors, 2010: Detection of supercooled liquid in mixed-phase clouds using radar Doppler spectra. *J. Geophys. Res.*, **115**, D19201, doi:10.1029/2009JD012884.

Mansell, E. R., and C. L. Ziegler, 2013: Aerosol effects on simulated storm electrification and precipitation in a two-moment bulk microphysics model. *J. Atmos. Sci.*, **70**, 2032–2050, doi:10.1175/JAS-D-12-0264.1.

——, ——, and E. Bruning, 2010: Simulated electrification of a small thunderstorm with two-moment bulk microphysics. *J. Atmos. Sci.*, **67**, 171–194, doi:10.1175/2009JAS2965.1.

Marcolli, C., 2017: Pre-activation of aerosol particles by ice preserved in pores. *Atmos. Chem. Phys.*, **17**, 1595–1622, doi:10.5194/acp-17-1595-2017.

Mason, B. J., 1996: The rapid glaciation of slightly supercooled cumulus clouds. *Quart. J. Roy. Meteor. Soc.*, **122**, 357–365, doi:10.1002/qj.49712253003.

——, 1998: The production of high ice-crystal concentrations in stratiform clouds. *Quart. J. Roy. Meteor. Soc.*, **124**, 353–356, doi:10.1002/qj.49712454516.

——, and J. Maybank, 1960: The fragmentation and electrification of freezing water drops. *Quart. J. Roy. Meteor. Soc.*, **86**, 176–185, doi:10.1002/qj.49708636806.

Matrosov, S. Y., R. F. Reinking, R. A. Kropfli, B. E. Martner, and B. W. Bartram, 2001: On the use of radar depolarization ratios for estimating shapes of ice hydrometeors in winter clouds. *J. Appl. Meteor.*, **40**, 479–490, doi:10.1175/1520-0450(2001)040<0479:OTUORD>2.0.CO;2.

McFarquhar, G., and Coauthors, 2017: Data analysis, interpretation, and presentation of in situ measurements. *Ice Formation and Evolution in Clouds and Precipitation: Measurement and Modeling Challenges*, *Meteor. Monogr.*, No. 58, Amer. Meteor. Soc., doi:10.1175/AMSMONOGRAPHS-D-16-0007.1.

Mizuno, H., and T. Matsuo, 1992: Collision between graupel particles: A field observation and theory. *J. Meteor. Soc. Japan*, **70**, 1037–1043.

Morrison, H., J. A. Curry, and V. Khvorostyanov, 2005: A new double-moment microphysics parameterization for application in cloud and climate models. Part I: Description. *J. Atmos. Sci.*, **62**, 1665–1677, doi:10.1175/JAS3446.1.

Mossop, S. C., 1985: Secondary ice particle production during rime growth. the effect of drop size distribution and rimer velocity. *Quart. J. Roy. Meteor. Soc.*, **111**, 1113–1124, doi:10.1002/qj.49711147012.

——, A. Ono, and E. R. Wishart, 1970: Ice particles in maritime clouds near Tasmania. *Quart. J. Roy. Meteor. Soc.*, **96**, 487–508, doi:10.1002/qj.49709640910.

——, J. L. Brownscombe, and G. J. Collins, 1974: The production of secondary ice particles during riming. *Quart. J. Roy. Meteor. Soc.*, **100**, 427–436, doi:10.1002/qj.49710042514.

Myagkov, A., P. Seifert, U. Wandinger, J. Bühl, and R. Engelmann, 2016: Relationship between temperature and apparent shape of pristine ice crystals derived from polarimetric cloud radar observations during the ACCEPT campaign. *Atmos. Meas. Tech.*, **9**, 3739–3754, doi:10.5194/amt-2015-365.

Oraltay, R. G., and J. Hallett, 1989: Evaporation and melting of ice crystals: A laboratory study. *Atmos. Res.*, **24**, 169–189, doi:10.1016/0169-8095(89)90044-6.

Oue, M., and Coauthors, 2015: Linear depolarization ratios of columnar ice crystals in a deep precipitating system over the Arctic observed by zenith-pointing Ka-band Doppler radar. *J. Appl. Meteor. Climatol.*, **54**, 1060–1068, doi:10.1175/JAMC-D-15-0012.1.

Ovtchinnikov, M. and Y. L. Kogan, 2000: An investigation of ice production mechanisms in small cumuliform clouds using a 3D model with explicit microphysics. Part I: Model description. *J. Atmos. Sci.*, **57**, 2989–3003, 10.1175/1520-0469(2000)057<2989:AIOIPM>2.0.CO;2.

Phillips, V. T. J., A. M. Blyth, P. R. A. Brown, T. W. Choularton, and J. Latham, 2001: The glaciation of a cumulus cloud over New Mexico. *Quart. J. Roy. Meteor. Soc.*, **127**, 1513–1534, doi:10.1002/qj.49712757503.

——, T. W. Choularton, A. J. Illingworth, R. J. Hogan, and P. R. Field, 2003: Simulations of the glaciation of a frontal mixed-phase cloud with the explicit microphysics model. *Quart. J. Roy. Meteor. Soc.*, **129**, 1351–1371, doi:10.1256/qj.02.100.

——, L. J. Donner, and S. T. Garner, 2007: Nucleation processes in deep convection simulated by a cloud-system-resolving model with double-moment bulk microphysics. *J. Atmos. Sci.*, **64**, 738–761, doi:10.1175/JAS3869.1.

Pruppacher, H. R., and J. D. Klett, 1997: *Microphysics of Clouds and Precipitation*. 2nd ed. Kluwer Academic, 954 pp.

Rangno, A., and P. Hobbs, 2001: Ice particles in stratiform clouds in the Arctic and possible mechanisms for the production of high ice concentrations. *J. Geophys. Res.*, **106**, 15 065–15 075, doi:10.1029/2000JD900286.

——, and ——, 2005: Microstructures and precipitation development in cumulus and small cumulonimbus clouds over the warm pool of the tropical Pacific Ocean. *Quart. J. Roy. Meteor. Soc.*, **131**, 639–673, doi:10.1256/qj.04.13.

Rasmussen, R. M., B. C. Bernstein, M. Murakami, G. Stossmeister, J. Reisner, and B. Stankov, 1995: The 1990 Valentine's Day Arctic outbreak. Part I: Mesoscale structure and evolution of a Colorado Front Range shallow upslope cloud. *J. Appl. Meteor.*, **34**, 1481–1511, doi:10.1175/1520-0450-34.7.1481.

Reisner, J., R. M. Rasmussen, and R. T. Bruintjes, 1998: Explicit forecasting of supercooled liquid water in winter storms using the MM5 mesoscale model. *Quart. J. Roy. Meteor. Soc.*, **124**, 1071–1107, doi:10.1002/qj.49712454804.

Rogers, D. C., and G. Vali, 1987: Ice crystal production by mountain surfaces. *J. Climate Appl. Meteor.*, **26**, 1152–1168, doi:10.1175/1520-0450(1987)026<1152:ICPBMS>2.0.CO;2.

Saleeby, S. M., and S. C. van den Heever, 2013: Developments in the CSU-RAMS aerosol model: Emissions, nucleation, regeneration, deposition, and radiation. *J. Appl. Meteor. Climatol.*, **52**, 2601–2622, doi:10.1175/JAMC-D-12-0312.1.

Sassen, K., 2005, Polarization in lidar. *Lidar*, C. Weitkamp, Ed., Springer, 19–42.

Saunders, C. P. R., and A. S. Hosseini, 2001: A laboratory study of the effect of velocity on Hallett–Mossop ice crystal multiplication. *Atmos. Res.*, **59–60**, 3–14, doi:10.1016/S0169-8095(01)00106-5.

Schaefer, V. J., and R. J. Cheng, 1971: The production of ice crystal fragments by sublimation and electrification. *J. Rech. Atmos.*, **5**, 5–10.

Scott, B. C., and P. V. Hobbs, 1977: A theoretical study of the evolution of mixed-phase cumulus clouds. *J. Atmos. Sci.*, **34**, 812–826, doi:10.1175/1520-0469(1977)034<0812:ATSOTE>2.0.CO;2.

Seifert, A., and K. D. Beheng, 2006: A two-moment cloud microphysics parameterization for mixed-phase clouds. Part 1: Model description. *Meteor. Atmos. Phys.*, **92**, 45–66, doi:10.1007/s00703-005-0112-4.

Sinclair, V. A., D. Moisseev, and A. von Lerber, 2016: How dual-polarization radar observations can be used to verify model representation of secondary ice. *J. Geophys. Res.*, **121**, 10,954–10,970, doi:10.1002/2016JD025381.

Stith, J. L., C. H. Twohy, P. J. DeMott, D. Baumgardner, T. Campos, R. Gao, and J. Anderson, 2011: Observations of ice nuclei and heterogeneous freezing in a western Pacific

extratropical storm. *Atmos. Chem. Phys.*, **11**, 6229–6243, doi:10.5194/acp-11-6229-2011.

Storelvmo, T., J. E. Kristjánsson, and U. Lohmann, 2008: Aerosol influence on mixed-phase clouds in CAM-Oslo. *J. Atmos. Sci.*, **65**, 3214–3230, doi:10.1175/2008JAS2430.1.

Sun, J. M., P. A. Ariya, H. G. Leighton, and M. K. Yau, 2010: Mystery of ice multiplication in warm-based precipitating shallow cumulus clouds. *Geophys. Res. Lett.*, **37**, L10802, doi:10.1029/2010GL042440.

——, ——, H. Leighton, and M. Yau, 2012: Modeling study of ice formation in warm-based precipitating shallow cumulus clouds. *J. Atmos. Sci.*, **69**, 3315–3335, doi:10.1175/JAS-D-11-0344.1.

Takahashi, T., Y. Nagao, and Y. Kushiyama, 1995: Possible high ice particle production during graupel–graupel collisions. *J. Atmos. Sci.*, **52**, 4523–4527, doi:10.1175/1520-0469(1995)052<4523:PHIPPD>2.0.CO;2.

Taylor, J. W., and Coauthors, 2016: Observations of cloud microphysics and ice formation during COPE. *Atmos. Chem. Phys.*, **16**, 799–826, doi:10.5194/acp-16-799-2016.

Thompson, G., and T. Eidhammer, 2014: A study of aerosol impacts on clouds and precipitation development in a large winter cyclone. *J. Atmos. Sci.*, **71**, 3636–3658, doi:10.1175/JAS-D-13-0305.1.

Vali, G., D. Leon, and J. R. Snider, 2012: Ground-layer snow clouds. *Quart. J. Roy. Meteor. Soc.*, **138**, 1507–1525, doi:10.1002/qj.1882.

Vardiman, L., 1978: The generation of secondary ice particles in clouds by crystal–crystal collisions. *J. Atmos. Sci.*, **35**, 2168–2180, doi:10.1175/1520-0469(1978)035<2168:TGOSIP>2.0.CO;2.

Verlinde, J., M. P. Rambukkange, E. E. Clothiaux, G. M. McFarquhar, and E. W. Eloranta, 2013: Arctic multilayered, mixed-phase cloud processes revealed in millimeter-wave cloud radar Doppler spectra. *J. Geophys. Res. Atmos.*, **118**, 13 199–13 213, doi:10.1002/2013JD020183.

Visagie, P. J., 1969: Pressures inside freezing water drops. *J. Glaciol.*, **8**, 301–309.

Wilson, D. R., A. J. Illingworth, and T. M. Blackman, 1997: Differential Doppler velocity: A radar parameter for characterizing hydrometeor size distributions. *J. Appl. Meteor.*, **36**, 649–663, doi:10.1175/1520-0450-36.6.649.

Woodley, W. L., G. Gordon, T. Henderson, B. Vonnegut, D. Rosenfeld, and A. Detwiler, 2003: Aircraft-produced ice particles (APIPs): Additional results and further insights. *J. Appl. Meteor.*, **42**, 640–651, doi:10.1175/1520-0450(2003)042<0640:AIPAAR>2.0.CO;2.

Yano, J.-I., and V. T. J. Phillips, 2011: Ice–ice collisions: An ice multiplication process in atmospheric clouds. *J. Atmos. Sci.*, **68**, 322–333, doi:10.1175/2010JAS3607.1.

——, ——, and V. Kannwade, 2016: Explosive ice multiplication by mechanical break-up in ice–ice collisions: A dynamical system-based study. *Quart. J. Roy. Meteor. Soc.*, **142**, 867–879, doi:10.1002/qj.2687.

Young, K. C., 1974: The role of contact nucleation in ice phase initiation in clouds. *J. Atmos. Sci.*, **31**, 768–776, doi:10.1175/1520-0469(1974)031<0768:TROCNI>2.0.CO;2.

Zawadzki, I., F. Fabry, and W. Szyrmer, 2001: Observations of supercooled water and secondary ice generation by a vertically pointing X-band Doppler radar. *Atmos. Res.*, **59-60**, 343–359, doi:10.1016/S0169-8095(01)00124-7.